Conditional Power and Rate Adaptation for MQAM/OFDM Systems Under CFO With Perfect and Imperfect Channel Estimation Errors

Zhicheng Dong, *Student Member, IEEE*, Pingzhi Fan, *Fellow, IEEE*, Erdal Panayirci, *Life Fellow, IEEE*, and Xianfu Lei, *Member, IEEE*

***Abstract*—In this paper, a new *conditional* power and rate adaptation scheme for orthogonal frequency-division multiplexing (OFDM) systems is proposed in the presence of carrier frequency offset (CFO), with perfect and imperfect channel state information (CSI). The conventional adaptive scheme is shown to be a special case of the conditionally adaptive scheme technique that enables the resulting nonconvex optimization problem, which is solved in a feasible way. It leads to a solution for optimal power adaptation that maximizes the spectral efficiency of an OFDM system using M-ary quadrature amplitude modulation (MQAM) under average power and instantaneous bit error rate (BER) constraints. Closed-form expressions for the average spectral efficiency (ASE) of adaptive OFDM systems are derived for perfect and imperfect CSI cases. The theoretical results and computer simulations show that range of the conditional adaptation becomes narrow and the performance of constant power and continuous rate is very close to that of the conditionally adaptive power and continuous rate for higher CFO or high signal-to-noise ratio (SNR) values.**

***Index Terms*—Average spectral efficiency (ASE), carrier frequency offset (CFO), conditional power and rate adaptation, intercarrier interference (ICI), orthogonal frequency-division multiplexing (OFDM).**

Manuscript received September 16, 2013; revised February 13, 2014; June 5, 2014; August 31, 2014; and October 16, 2014; accepted November 5, 2014. Date of publication December 4, 2014; date of current version November 10, 2015. This work was supported in part by the National Basic Research Program of China under Grant 2012CB316100, by the National Science Foundation of China under Grant 61471302, by the 111 Project under Grant 111-2-14, by the Fundamental Research Funds for the Central Universities under Grant SWJTU12ZT02/2682014ZT11, and by the 2013 Doctoral Innovation Funds of Southwest Jiaotong University and the Fundamental Research Funds for the Central Universities. The review of this paper was coordinated by Dr. J.-C. Chen.

Z. Dong is with Key Laboratory of Information Coding and Transmission, Southwest Jiaotong University, Chengdu 610031, China, and also with the School of Engineering, Tibet University, Lhasa 850000, China (e-mail: dongzc666@163.com).

P. Fan is with Key Laboratory of Information Coding and Transmission, Southwest Jiaotong University, Chengdu 610031, China (e-mail: pzfan@swjtu.edu.cn).

E. Panayirci is with the Department of Electrical and Electronics Engineering, Kadir Has University, Istanbul 34230, Turkey (e-mail: eepanay@khas.edu.tr).

X. Lei is with the Department of Electrical and Computer Engineering, Utah State University, Logan, UT 84322-4120 USA (e-mail: xflei81@yahoo.com.cn).

Color versions of one or more of the figures in this paper are available online at http://ieeexplore.ieee.org.

Digital Object Identifier 10.1109/TVT.2014.2377153

I. Introduction

Orthogonal frequency-division multiplexing (OFDM) has been shown to be an effective technique to overcome the intersymbol interference (ISI) caused by frequency-selective fading with a simple transceiver structure. It has emerged as the leading transmission technique for a wide range of wireless communication standards [1] such as the IEEE 802.16 family, which is well known as Mobile Worldwide Interoperability Microwave Systems for the Next-Generation Wireless Communication Systems (WiMAX) and the Third-Generation Partnership Project (3GPP) in the form of its Long-Term Evolution (LTE) project. Both systems employ orthogonal frequency-division multiplexing/multiple access (OFDMA) and a new single-carrier frequency-division multiple-access format. To promote the IEEE 802.16 and LTE standards, recently, a high-mobility feature was introduced [IEEE 802.16m, LTE Advanced] to enable mobile broadband services at vehicular speeds beyond 120 km/h.

However, OFDM is more sensitive to frequency synchronization errors than the single-carrier systems. Carrier frequency offset (CFO) in OFDM systems results in a loss of subchannel orthogonality, which leads to interchannel interference (ICI). ICI will degrade the spectral efficiency of the system [2]. The impact of CFO on OFDM systems was investigated in [3], [4] and references therein. Cheon and Dong [3] studied the performance degradation due to the channel estimation errors and CFO in OFDM-based local area network (LAN) systems. Rugini and Banelli derived the BER of OFDM systems with CFO in frequency-selective Rician and Rayleigh fading channels [4].

In conventional OFDM, the same modulation scheme is employed and the same power is allocated on all subchannels. However, severely faded subchannels can degrade the performance substantially. Adaptive modulation is a promising technique to improve the performance by increasing the data rate that can be reliably transmitted over fading channels. For this reason, some form of adaptive modulation is being employed in many next-generation wireless communication systems. Adaptive modulation adapts the transmitted signal to match the frequency-selective fading channel, which is called adaptive bit loading. Transmit power, data rate, instantaneous bit error rate (BER), and channel code rate in each subchannel can be adapted relative to the channel [5]. However, to achieve the performance advantage of adaptive modulation, accurate receiver channel state information (CSI) is required at the transmitter [6]–[8]. The impact of channel estimation errors on adaptive modulation schemes has been investigated in [9] and [10]. Adaptive transmission in the presence of imperfect CSI for OFDM systems has also been studied in [11] and [12]. In [13] and [14], the use of adaptive bit loading in conjunction with an adaptive subcarrier bandwidth has been proposed. However, adaptive power distribution and imperfect CSI were not considered. For the types of constraints on the fairness, the sum throughput maximization with access proportional fairness is studied in [15] for downlink OFDMA channels. In [16], an algorithm is proposed for multiple-input–multiple-output (MIMO) OFDM system that can achieve almost the maximum sum capacity while keeping the proportional fairness.

On the other hand, there are only a few works existing in the literature on OFDM-based adaptive modulation schemes with CFO and imperfect CSI [3], [17]–[20]. In [3], the instantaneous and average effective SNR and average BER of OFDM systems are derived in the presence of CFO and the channel estimation errors for Rayleigh fading channels. A new robust algorithm for the problem of achievable throughput maximization in power line networks systems in the presence of interference have been devised in [20]. In [17] and [18], a power and rate adaptive scheme for M-ary quadrature amplitude modulation (MQAM)/OFDM under a very fast fading channel with perfect and imperfect CSI was studied as opposed to the scheme used in this paper, which mainly deals with power and rate adaptation in the presence of CFO. The formulation and, in particular, the optimization problems leading to the solutions in [17] and [18] and this paper are very different. Mainly, a new BER model is formulated in [17] and [18] for OFDM systems under a fast fading channel in which the ICI is determined by the largest transmit power to meet the BER constraint. In these papers, it has been simply assumed that the largest transmit power was equal to the transmit power when the channel gain approaches to infinity and used a conventional convex optimization technique to obtain both the optimal power and bit distributions. Consequently, these studies have not considered the optimization problem, taking into account the largest transmit power, the power distribution, and the bit adaptation, jointly. Therefore, the scheme investigated in these studies does not yield an optimal solution. On the other hand, this paper is concerned with power and rate adaptation in the presence of a CFO, and a conditionally adaptive scheme is proposed to solve the resulting nonconvex optimization problem in a feasible way. The spectral efficiency of adaptive MQAM/OFDM systems with CFO in the presence of perfect and imperfect CSI over Rayleigh fading channels was investigated in [19]. The optimal adaptation on each OFDM subchannel considered in [19] generally leads to a nonconvex log-fractional optimization problem whose solution is mathematically intractable, in general. This is mainly due to the fact that the instantaneous transmit power carried by OFDM subcarriers is not the same and the objective function needs the knowledge of other subchannel power for the ICI term, which are very difficult to determine during the adaptation. In [19], a feasible solution is proposed by assuming the ICI power of the subchannel to be optimized is approximated by its own power.

This paper is concerned with continuous power and rate adaptation of OFDM systems with CFO in the presence of perfect and imperfect CSI, under average power and instantaneous BER constraint. The main contributions of this paper can be stated as follows.

- Based on the new BER model, closed-form analytical expressions are obtained for optimal power distribution, maximum bit load, and average spectral efficiency (ASE) under both perfect and imperfect CSI cases. It is shown that the proposed adaptive scheme with perfect CSI is a special case for the imperfect CSI.
- Based on the expressions derived for optimal power distribution and maximum bit load, a new adaptive scheme called the *conditionally adaptive scheme* is proposed for the first time in the literature, which also leads to two different special cases. Namely, the *complete adaptive scheme* and the *uniform power distribution*. When CFO or channel estimation error is small, the *conditionally adaptive scheme* turns out to be the *complete adaptive scheme*. On the other hand, when the CFO or channel estimation error is large, the *conditionally adaptive scheme* tends to the *uniform power distribution*. These results are invaluable in simplifying the system design under communication scenarios with only negligible system degradation.
- The new optimization formulation proposed in this paper is quite different from the conventional approaches appeared in the literature, which mostly lead to a convex optimization problem. A new constraint, namely *variable largest transmit power*, which is included in the formulation of the problem, makes the resulting optimization nonconvex. Using the linear-fractional programming, it is solved by transforming the nonconvex optimization into a convex one and proved that the resulting solution is optimal. To our knowledge, the new method proposed in the paper, which solves the power and rate adaptation in communications systems with CFO, has not previously appeared in the literature. We believe the same technique could be extended easily to other interference scenarios in communications successfully.
- A novel method is provided to prove that the proposed scheme can meet the BER constraint, which is a function of the "mismatch" between the approximation model and the exact model. The new method can also be extended to investigate the performances of the similar communication scenarios with interference.

The remainder of this paper is organized as follows. Section II introduces an OFDM system model based on CFO. Section III discusses the adaptive OFDM systems under CFO with perfect channel estimation. The adaptive OFDM systems under CFO with imperfect channel estimation are discussed in Section IV. Finally, in Section V, the simulation and numerical results are presented, along with some concluding remarks.

II. System Model

We consider an OFDM system with K subcarriers. At the transmitter, N out of K subcarriers are actively employed to transmit data symbols, and nothing is transmitted from the remaining $K-N$ carriers. Each active subcarrier is modulated by a data symbol $X[k]$, where k represents the OFDM subcarrier index. After taking a K-point inverse fast Fourier transform of the data sequence and adding a cyclic prefix (CP) of duration $T_{\rm CP}$ before transmission, to avoid ISI, for a given frequency offset ν, the received OFDM symbol at the input of the discrete Fourier transform can be expressed as [3], [19]

$$y[n] = \frac{1}{\sqrt{K}} \sum_{k=0}^{K-1} H[k]X[k]e^{2\pi n(k+\nu)/K} + w[n] \tag{1}$$

where $H[k]$ denotes the discrete frequency response of the channel at the kth subcarrier, and $w[n]$ is the additive zero-mean complex Gaussian noise with variance σ_w^2. The kth subcarrier output of the DFT during one OFDM symbol can be expressed as

$$\begin{aligned} Y[k] &= \frac{1}{\sqrt{K}} \sum_{n=0}^{N-1} y[n]e^{-j2\pi nk/N} + W[k] \\ &= H_k^\nu X[k] + I_k + W[k] \end{aligned} \tag{2}$$

where $W[k]$ is a frequency-domain additive Gaussian noise on the kth subcarrier; I_k is the ICI caused by the frequency offset, which is given by [2], [3], [21]

$$\begin{aligned} I_k = &\sum_{m\in\kappa, m\neq k} H[m]X[m]\sin\pi\nu \cdot e^{j(\pi\nu(k-1)/K)} \\ &/\left(K\sin\left(\pi(m-k+\nu)/K\right)\right) e^{-j(\pi(m-k)/K)} \end{aligned} \tag{3}$$

with $\kappa = \{0, 1, \ldots, K-1\}$; and H_k^ν denotes the distorted channel response, which is written as

$$H_k^\nu = \frac{H[k]\sin\pi\nu}{K\sin(\pi\nu/K)} e^{j(\pi\nu(K-1)/K)}. \tag{4}$$

From (3), the ICI power of the kth OFDM subcarrier can be obtained as

$$P_{\rm ICI}^{(k)} = E\left\{|I_k|^2\right\} = \sum_{m\in\kappa, m\neq k} E\left\{|X[m]|^2\right\} \rho_{k,m} \tag{5}$$

where $E\{.\}$ denotes expectation, and

$$\rho_{k,m} = \left(\frac{\sin\pi\nu}{K\sin\left(\pi(m-k+\nu)/K\right)}\right)^2.$$

Since data on each subcarrier are uncorrelated, it follows easily from (5) that the normalized ICI power σ_ν^2, which is adopted in this paper, is $\sigma_\nu^2 = P_{\rm ICI}^{(K)}/E\{|X[m]|^2\} \approx (\pi\nu)^2/3$, [3], [19].

III. Adaptive Orthogonal Frequency Division Multiplexing Systems Under Carrier Frequency Offset

Let $\overline{S}$ denote the average transmitted signal power on each OFDM subcarrier, i.e., $E\{|X[k]|^2\} = \overline{S}$. With appropriate scaling of $\overline{S}$, we can assume that the average channel power gain on each subcarrier is unity. That is, $E\{|H[k]|^2\} = 1$. For fixed power allocation (constant transmit power on each subcarrier), the instantaneous effective SNR, for fixed power allocation, is shown to be

$$\gamma_e(k) = \frac{\overline{S}\,|H[k]|^2}{\overline{S}\sigma_\nu^2 + \sigma_w^2} = \frac{\gamma[k]}{\overline{\gamma}\sigma_\nu^2 + 1} \tag{6}$$

where $\gamma[k] \triangleq \overline{\gamma}|H[k]|^2$ is called the instantaneous received SNR of the kth subcarrier, and $\overline{\gamma} = \overline{S}/\sigma_w^2$ is the average SNR when there is no ICI. Similarly, for different power levels $s(\gamma[k])$ allocated to each OFDM subchannels, which are functions of $\gamma[k]$, the effective SNR in the kth subchannel can be expressed as

$$\widetilde{\gamma}_e\left(s\left(\gamma[k]\right)\right) = \frac{s\left(\gamma[k]\right)|H[k]|^2}{\overline{S}P_N^{(k)} + \sigma_w^2} = \frac{\gamma[k]\frac{s(\gamma[k])}{\overline{S}}}{\overline{\gamma}P_N^{(k)} + 1} \tag{7}$$

where $P_N^{(k)}$ is the normalized ICI power (variance) of the kth subcarrier. From (5), it follows that

$$P_N^{(k)} = \sum_{m\in\kappa, m\neq k} \frac{s\left(\gamma[m]\right)}{\overline{S}} \rho_{k,m}. \tag{8}$$

In this paper, we investigate the continuous power and transmission rate adaptation at the transmitter by maximizing the ASE in the presence of a CFO. The ASE of an OFDM transmission scheme is defined as $C_{\rm ASE} = E_{(\gamma[k])}\sum_{k\in K}\beta(\gamma[k])/BT_{\rm SYM}$, where B is the total bandwidth, and $T_{\rm SYM}$ denotes the duration of an OFDM symbol. This results in a subchannel spacing of $\Delta f = B/K$ and $T_{\rm SYM} = 1/\Delta f = K/B$. We assume that a Nyquist filtering is employed in the system with the sampling duration $T_s = 1/B$ [13], [14], [19]. If we neglect the impact of CP on ASE, the ASE becomes $C_{\rm ASE} = E_{(\gamma[k])}(1/K\sum_{k\in K}\beta(\gamma[k]))$. When the discrete frequency responses of the channel are independent identically distributed (i.i.d.) random variables with probability density function (pdf) $p(\cdot)$, [11], [19], the ASE can be expressed as

$$C_{\rm ASE} = \int_0^\infty \beta\left(\gamma[k]\right)p\left(\gamma[k]\right)d\gamma[k] \text{ bits/s/Hz.} \tag{9}$$

We also assume an average transmit power constraint given by

$$E_{\gamma[k]}\left\{s\left(\gamma[k]\right)\right\} = \int_0^\infty s\left(\gamma[k]\right)p\left(\gamma[k]\right)d\gamma[k] = \overline{S}. \tag{10}$$

As a function of instantaneous effective4455 SNR, i.e., $\widetilde{\gamma}_e(s(\gamma[k]))$, the $\mathrm{BER}(\gamma[k])$, corresponding to a square MQAM

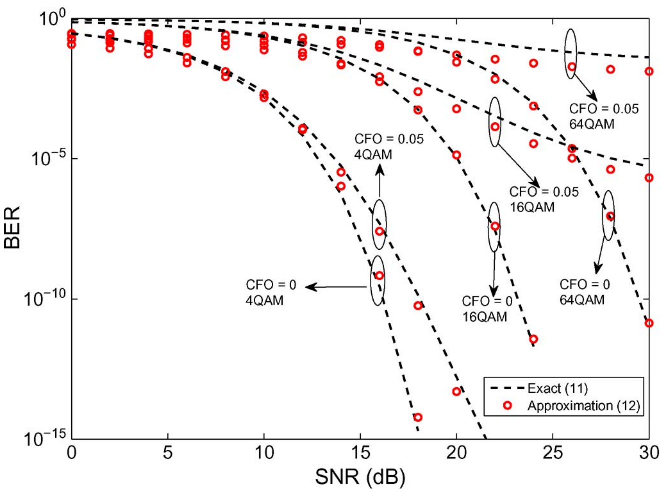

Fig. 1. BER approximations for MQAM with different CFO values.

signaling with Gray bit mapping for each subchannel under CFO, can be expressed as [22]

$$\begin{aligned}\mathrm{BER}\left(\gamma[k]\right) &= 1-\left[1-\frac{\sqrt{2^{\beta(\gamma[k])}}-1}{\sqrt{2^{\beta(\gamma[k])}}}\times 2Q\left(\sqrt{\frac{3\widetilde{\gamma}_e\left(s\left(\gamma[k]\right)\right)}{\left(2^{\beta(\gamma[k])}-1\right)}}\right)\right]^2\\ &= \frac{4}{\beta\left(\gamma[k]\right)}\left(1-\frac{1}{\sqrt{2^{\beta(\gamma[k])}}}\right)\\ &\quad\times\sum_{i=0}^{\sqrt{2^{\beta(\gamma[k])}}/2-1} Q\left((2i+1)\sqrt{\frac{3\widetilde{\gamma}_e\left(s(\gamma[k])\right)\beta\left(\gamma[k]\right)}{\left(2^{\beta(\gamma[k])}-1\right)}}\right)\end{aligned} \tag{11}$$

where $\widetilde{\gamma}_e(s(\gamma[k]))$ is given in (7). $Q(\boldsymbol{.})$ denotes the Gaussian Q-function, and is defined as $1/\sqrt{2\pi}\int_x^\infty e^{-t^2/2}\,dt$. This expression is not easily differentiable or invertible in its power $s(\gamma[k])$ and rate $\beta(\gamma[k])$. A tight approximate BER expression for the square MQAM with Gray mapping is as follows [5], [11]–[14], [19], [23]:

$$\mathrm{BER}\left(\gamma[k]\right)\approx C_1\exp\left(\frac{-C_2\widetilde{\gamma}_e\left(s\left(\gamma[k]\right)\right)}{2^{\beta(\gamma[k])}-1}\right) \tag{12}$$

where $C_1 = 0.3$, and $C_2 = 1.5$. The approximation is tight for $M \geq 4$ and $0 \leq \overline{\gamma} \leq 30$ dB when $CFO = 0$ [5], [23]. Considering the effect of CFO, the approximation is tight for $M \geq 4$, $5 \leq \overline{\gamma} \leq 30$ dB, and $CFO \leq 0.3$ with fixed power allocation. In Fig. 1, we plot the BER as a function of average received SNR with fixed power allocation. The figure shows that the approximation (12) employed in this paper achieves an excellent fit to the exact BER formula (11).

We now derive the optimal continuous rate and power adaptation to maximize the spectral efficiency in (9) subject to the average power constraint (10) and an instantaneous BER constraint $\mathrm{BER}(\gamma[k]) \leq \epsilon$. Taking into account $\widetilde{\gamma}_e(s(\gamma[k])$ in (7) and inverting (12), the bit load size $\beta(\gamma[k])$ for each subchannel can be expressed as a function of the variable power on each subcarrier $s(\gamma[k])$ and the fixed BER ϵ $(\mathrm{BER}(\gamma[k]) = \epsilon)$ as

$$\beta\left(\gamma[k]\right)=\log_2\left(1+\frac{\left(-1.5\varphi/\ln(\varepsilon/0.3)\right)\gamma[k]\frac{s(\gamma[k])}{\overline{S}}}{\overline{\gamma}P_N^{(k)}+1}\right) \tag{13}$$

where $\widetilde{\gamma}_e(s(\gamma[k]))$ is given by (7), and $\varphi = (\sin(\pi\nu)/(K\sin(\pi\nu/K)))^2 \approx (\sin(\pi\nu)/(\pi\nu))^2$ [2], [3], [21]. It can be easily seen from (8) and (13) that maximizing the ASE of the kth subchannel (9) in an adaptive OFDM system, under the average signal power constraint (10), needs the knowledge of the other subcarrier powers $s(\gamma[m])/\overline{S}$, $m = 0, 1, \ldots, K-1$, which makes the solution of the optimization problem mathematically intractable. Note that it is very difficult to determine the exact ICI power $P_N^{(k)}$ in (8) when instantaneous transmit power carried by OFDM subcarriers is not the same during the power adaptation. To obtain a feasible solution, [19] assumes that the normalized ICI power of the kth subchannel can be determined by its own power, i.e., $P_N^{(k)} = (s(\gamma[k])/\overline{S})\sigma_\nu^2$. On the other hand, in this paper, we propose an upper bound for $P_N^{(k)}$ in terms of the largest transmit normalized power $s_{\max} = \max_{m\in\kappa}\{s(\gamma[m])/\overline{S}\}$. As explained in the following, the BER constraint, in this case, is always met since the power transmitted by other subcarriers is less than or equal to $s_{\max}$.

The approximate ICI power affects the BER of the adaptive system. At the transmitter, the approximate ICI power model is employed to determine the constellation type and the power of the signal to be sent. The transmit power and the rate are adapted as $s(\gamma[k])$ and $\beta(\gamma[k])$ based on the approximate ICI power instead of $\hat{s}(\gamma[k])$ and $\hat{\beta}(\gamma[k])$ based on the exact ICI power. At the receiver, the approximation ICI power model is used to determine the signal constellation and the power level, as well as to scale the decision regions of the MQAM demodulator corresponding to that constellation and power. However, the real instantaneous BER is decided by the exact ICI power. Thus, the decision regions of the MQAM demodulator will be scaled according to the approximate ICI power instead of the exact ICI power, which would cause a change in the target BER. Suppose now the transmitter adapts its power and rate relative to a target $\mathrm{BER} = \epsilon$ based on the approximate ICI power instead of the true ICI power. Then, from (12) and (7), the instantaneous BER, which becomes a function of the "mismatch" between the approximation ICI power and the exact ICI power, can be expressed as

$$\begin{aligned}&\mathrm{BER}\left(\gamma[k]\right)\left(P_{\mathrm{ICIEX}}, P_{\mathrm{ICIAP}}\right)\\ &\quad= C_1\exp\left(\frac{-C_2\gamma[k]\frac{s(\gamma[k])}{\overline{S}}}{\left(2^{\beta(\gamma[k])}-1\right)\left(\overline{\gamma}P_N^{(k)}+1\right)}\right)\\ &\quad= C_1(\epsilon/C_1)^\chi\end{aligned} \tag{14}$$

where $P_N^{(k)}$ is given in (8). χ is the mismatch value, which is defined as $\chi \triangleq P_{\mathrm{ICIAP}}/P_{\mathrm{ICIEX}}$. P_{ICIEX} and P_{ICIAP} denote the exact ICI power and approximation ICI power, respectively. P_{ICIEX} is equal to $\overline{\gamma}P_N^{(k)}$, and P_{ICIAP} has different values for different approximation ICI power schemes. For instance, P_{ICIAP} is equal to $s_{\max}\sigma_\nu^2\overline{\gamma}$ in the proposed scheme. For $\chi = 1$, (14) reduces to the target BER ϵ. For $\chi \neq 1$, $\chi < 1$

yields an increase and $\chi > 1$ a decrease in the target BER. From (14), $\chi > 1$ implies that the constraint of BER is always met since $\text{BER}(\gamma[k]) = \epsilon'$, where $\epsilon' = C_1(\epsilon/C_1)^{\chi} < \epsilon$. On the contrary, by the same argument, $\chi < 1$ implies that the constraint of BER is never met.

We now prove that our proposed scheme does meet the BER constraint by showing that $\chi \geq 1$. Since $P_{\text{ICIEX}} = \overline{\gamma} P_N^{(k)}$, $P_{\text{ICIAP}} = s_{\max}\sigma_\nu^2\overline{\gamma}$ with $P_N^{(k)}$ given by (8), it follows that

$$\chi = \frac{P_{\text{ICIAP}}}{P_{\text{ICIEX}}} = \frac{s_{\max}\sigma_\nu^2\overline{\gamma}}{\overline{\gamma}\sum\limits_{m\in\kappa, m\neq k}\frac{s(\gamma[m])}{\overline{S}}\rho_{k,m}}. \tag{15}$$

Since in our scheme, $s_{\max} \geq s(\gamma[m])/\overline{S},\ \forall m \in K$, and $\sigma_\nu^2 = \sum_{m\in\kappa,m\neq k}\rho_{k,m}$ in (5), it follows from (15) that

$$\chi \geq \frac{s_{\max}\sigma_\nu^2\overline{\gamma}}{\overline{\gamma}\sum\limits_{m\in\kappa, m\neq k} s_{\max}\rho_{k,m}} = 1$$

which implies the proposed scheme can meet the BER constraint.

Consequently, employing the normalized ICI power, $P_N^{(k)}$ in (8), determined by $s_{\max}$, the maximum bit load size $\beta(\gamma[k])$ for each subchannel can be expressed from (13) as follows:

$$\beta(\gamma[k]) = \log_2\left(1 + \frac{a\gamma[k]s(\gamma[k])}{s_{\max}b + 1}\right) \tag{16}$$

where $a = -15\varphi/(\overline{S}\ln(\varepsilon/0.3)),\ b = \sigma_\nu^2\overline{\gamma}$.

We now consider the following constrained optimization problem to solve the power and rate adaptation problem:

$$\max_{s(\gamma[k]), s_{\max}} \int \beta(\gamma[k])\, p_{\gamma[k]}(\gamma[k])\, d\gamma[k] \tag{17a}$$

subject to

$$E_{\gamma[k]}\{s(\gamma[k])\} = \overline{S} \qquad \forall k \in \kappa \tag{17b}$$
$$0 \leq s(\gamma[k]) \leq s_{\max}\overline{S} \qquad \forall k \in \kappa \tag{17c}$$
$$\text{BER}(\gamma([k])) \leq \varepsilon \qquad \forall k \in \kappa. \tag{17d}$$

The given constraint optimization problem is not convex. However, it is in the form of a log-linear-fractional model [24], [25]. In Appendix A, using the linear-fractional programming, the problem is solved by transforming it into a convex optimization, resulting in the following optimal power adaptation:

$$\frac{s(\gamma[k])}{\overline{S}} = \begin{cases} \frac{s_{\max}b+1}{\ln(2)\lambda(z)\overline{S}} - \frac{s_{\max}b+1}{a\gamma[k]\overline{S}} & \gamma_0 \leq \gamma[k] \leq \gamma_1 \quad \forall k \in K \\ s_{\max} & \gamma[k] \geq \gamma_1 \quad \forall k \in \kappa \end{cases} \tag{18}$$

where $z = (s_{\max}b + 1)^{-1},\ \lambda(z)$ is the Lagrange multiplier, and

$$\gamma_0 = \ln(2)\lambda(z)/a \tag{19}$$

$$\gamma_1 = \frac{1}{a\left(1/(\ln(2)\lambda(z)) - (s_{\max}/(s_{\max}b+1))\,\overline{S}\right)}. \tag{20}$$

The values of $s_{\max}$ and the Lagrangian $\lambda(z)$ are found numerically based on (45). The details are described in Appendix A. Note that the average power (17b) and BER constraint (17d) are satisfied.

We call our method *conditionally adaptive scheme* since transmission power is adapted relative to channel variations in $[\gamma_0, \gamma_1]$ and becomes constant in $(\gamma_1, \infty]$. γ_0 and γ_1, which are defined in (19) and (20), are optimized thresholds for $\gamma[k]$, below which, the channel is not used and above which, the channel is used with a constant transmit power, respectively. On the other hand, the scheme proposed in [5] and [23] is a *complete adaptive scheme* since transmission power is adapted relative to channel variations over the whole range of the channel conditions.

It follows from (18) that $\lim_{\gamma[k]\to\infty}(s(\gamma[k])/\overline{S}) = (s_{\max}b + 1))/(\ln(2)\lambda(z)\overline{S})$. Consequently, if there is no limit for the largest power, the power adaptation is realized by the complete adaptive scheme. However, since ICI is decided by the largest power $s_{\max}$, there is a tradeoff between the adaptive scheme and the ICI as follows.

1) If $s_{\max} > (s_{\max}b + 1)/(\ln(2)\lambda(z)\overline{S})$, the ICI is overestimated, and the ASE decreases as the $s_{\max}$ increases.
2) If $1 < s_{\max} \leq (s_{\max}b + 1)/\ln(2)\lambda(z)\overline{S}$, the optimal $s_{\max}$ equals to $(1/z - 1)/b$, as shown in Appendix A.
3) $s_{\max} = 1$, which means a uniform power distribution.

The proposed scheme includes two special cases.

1) When $\gamma_0 = \gamma_1 = 0$, (18) becomes $s(\gamma[k])/\overline{S} = 1$ for $\gamma[k] \geq 0$, which means a uniform power distribution.
2) When $b = 0$ (CFO = 0), it can be shown from (20) that $\gamma_1 = \infty$, and thus, (18) reduces to $s(\gamma[k])/\overline{S} = (1/\ln(2)\lambda(z)\overline{S}) - (1/a\gamma[k]\overline{S})$, which has been investigated in [5] and [23]. Since there is no ICI, consequently, our adaptive scheme turns out to be a complete adaptive scheme.

From (13) and (18), the optimal bit rate adaptation on each subcarrier can be obtained as follows:

$$\beta(\gamma[k]) = \begin{cases} \log_2\left(\frac{a\gamma[k]}{\lambda(z)\ln(2)}\right), & \gamma_0 \leq \gamma[k] \leq \gamma_1 \quad \forall k \in \kappa \\ \log_2\left(1 + \frac{s_{\max}a\overline{S}\gamma[k]}{1+s_{\max}b}\right), & \gamma[k] \geq \gamma_1 \quad \forall k \in \kappa. \end{cases} \tag{21}$$

A closed-form expression for the optimal ASE can be obtained from (9) and (21), and by using the exponential pdf for $\gamma[k]$ with mean $\overline{S}$. The final result is given as follows, and the details are presented in Appendix B:

$$\begin{aligned} C_{\text{ASE}} = &\frac{1}{\ln(2)}\exp(-\gamma_0/\overline{S}) \\ &\times \left(\ln(\gamma_0 a/(\ln(2)\lambda(z))) + Ei(1, \gamma_0/\overline{S})\exp(\gamma_0/\overline{S})\right) \\ &- \frac{1}{\ln(2)}\exp(-\gamma_1/\overline{S}) \\ &\times \left(\ln(\gamma_1 a/(\ln(2)\lambda(z))) + Ei(1, \gamma_1/\overline{S})\exp(\gamma_1/\overline{S})\right) \\ &+ \frac{\exp(-\gamma_1/\overline{S})}{\ln(2)}(\log(1 + C\gamma_1) \\ &+ Ei\left(1, \frac{1 + C\gamma_1}{C\overline{S}}\right)\exp\left(1 + \frac{1 + C\gamma_1}{C\overline{S}}\right) \end{aligned} \tag{22}$$

where $C = a(1 - z)\overline{S}/b$, and z and $\lambda(z)$ can be calculated as explained in Appendix A.

IV. Adaptive Orthogonal Frequency Division Multiplexing Systems Under Carrier Frequency Offset With Imperfect Channel Estimation

In practice, it is impossible to obtain perfect channel information due to noisy channel estimation. Here, we investigate the performance degradation in terms of spectral efficiency in the presence of an imperfect CSI. Based on the BER expressions in (12), a new BER expression for continuous rate is presented for the case of imperfect CSI. Since the instantaneous BER of each subcarrier depends on the perfect CSI, which is assumed unknown, it is not possible to fix the exact instantaneous BER to be the target value. However, we can use the conditional expectation of $\text{BER}(\gamma[k])$, given $\gamma'[k]$, as follows:

$$\overline{\text{BER}}\left(\gamma'[k]\right) \triangleq E\left\{\text{BER}\left(\gamma[k]\right) \mid \gamma'[k]\right\}. \tag{23}$$

From (12) and (23), the average BER with imperfect channel estimation can be obtained by

$$\overline{\text{BER}}\left(\gamma'[k]\right) = \int_0^\infty 0.3\exp\left(\frac{-1.5\varphi\gamma[k]\frac{s(\gamma'[k])}{\overline{S}}}{\left(2^{\beta(\gamma[k])}-1\right)\left(s_{\max}\sigma_\nu^2\overline{\gamma}+1\right)}\right) \times p\left(\gamma[k] \mid \gamma'[k]\right) d\gamma[k]. \tag{24}$$

Assuming pilot-assisted MMSE-based channel estimation at the receiver, the conditional pdf of $\gamma[k]$ given $\gamma'[k]$ over Rayleigh-fading channels can be expressed as [12], [19]

$$p\left(\gamma[k] \mid \gamma'[k]\right) = \frac{1}{(1-\rho)\overline{\gamma}} I_0\left(2\frac{\sqrt{\rho}}{1-\rho}\sqrt{\frac{\gamma[k]\gamma'[k]}{\overline{\gamma}\overline{\gamma'[k]}}}\right) \times \exp\left\{\frac{-1}{1-\rho}\left(\frac{\gamma[k]}{\overline{\gamma}} + \frac{\gamma'[k]\rho}{\overline{\gamma'[k]}}\right)\right\}$$

where $\rho \in [0,1]$ is the correlation coefficient between $\gamma[k]$ and $\gamma'[k]$, and $\overline{\gamma'[k]}$ is the expectation of $\gamma'[k]$. $I_0(\cdot)$ is the zeroth-order modified Bessel function of the first kind. Taking the integral analytically in (24), the average BER can be obtained as follows:

$$\overline{\text{BER}}\left(\gamma'[k]\right) = 0.3\phi_\nu\left(\gamma'[k]\right) \times \exp\left\{\frac{-\rho}{1-\rho}\frac{\gamma'[k]}{\overline{\gamma'[k]}}\left(1-\phi_\nu\left(\gamma'[k]\right)\right)\right\} \tag{25}$$

where $\phi_\nu(\gamma'[k])$ is defined as

$$\phi_\nu\left(\gamma'[k]\right) = \frac{1}{\left(1+\frac{1.5\varphi(1-\rho)\overline{\gamma}s(\gamma'[k])/\overline{S}}{\left(2^{\beta(\gamma'[k])}-1\right)\left(s_{\max}\sigma_\nu^2\overline{\gamma}+1\right)}\right)}. \tag{26}$$

For the instantaneous BER target, $\text{BER}([\gamma[k]]) = \varepsilon$, it follows from (25) that

$$0.3\phi_\nu\left(\gamma'[k]\right) e^{\left\{-\frac{\rho}{1-\rho}\frac{\gamma'[k]}{\overline{\gamma'[k]}}\left(1-\phi_\nu(\gamma'[k])\right)\right\}} = \varepsilon. \tag{27}$$

$\phi_\nu(\gamma'[k])$ in (26) can be approximated by [12], [19]

$$f_\nu\left(\gamma'[k]\right) = 1 + \frac{(1-\rho)\overline{\gamma'[k]}}{\rho\gamma'[k]}\log\left(\varepsilon/0.3\right).$$

By substituting $f_\nu(\cdot)$ for $\phi_\nu(\cdot)$ in (26), the following relation between the power and rate of the kth subcarrier can be derived in (28):

$$\beta\left(\gamma'[k]\right) = \log_2\left(1+\frac{a\left[\rho\gamma'[k]+(1-\rho)\overline{\gamma'[k]}\ln\left(\varepsilon/0.3\right)\right]s(\gamma'[k])}{s_{\max}b+1}\right). \tag{28}$$

Similar to the perfect CSI case investigated in Section III, the optimal power adaptation is obtained by solving the constraint optimization problem with the modified Lagrangian

$$J\left(\gamma'[k]\right) = \int \beta\left(\gamma'[k]\right) p_{\gamma'[k]}\left(\gamma'[k]\right) d\gamma'[k] - \lambda(z)\int s\left(\gamma'[k]\right)/\overline{S} \times p_{\gamma'[k]}\left(\gamma'[k]\right) d\gamma'[k] \tag{29}$$

where $z = (s_{\max}b+1)^{-1}$, and $\lambda(z)$ is the Lagrange multiplier. Similar to the derivations in Appendix A for the perfect CSI case, the final solution for optimal power allocation on each subcarrier can be obtained in (30), shown at the bottom of the page, where

$$\gamma'_0 = \left(\ln(2)\lambda(z) - a(1-\rho)\overline{\gamma'[k]}\ln(\varepsilon/0.3)\right)/(a\rho)$$

$$\gamma'_1 = 1/\left(a\rho\left(1/\left(\ln(2)\lambda(z)\right)\right) - \left(s_{\max}/(s_{\max}b+1)\overline{S}\right)\right) - (1-\rho)\overline{\gamma'[k]}\ln(\varepsilon/0.3)/\rho$$

and γ'_0 and γ'_1 are the optimized thresholds for $\gamma'[k]$, below which, the channel is not used and above which, the channel is used with some fixed transmit power, respectively. With a perfect CSI, i.e., $\rho = 1$, then γ'_0 degenerates to γ_0 in (19), γ'_1 degenerates to γ_1 in (20), and optimal power allocation $s(\gamma'[k])/\overline{S}$ degenerates to $s(\gamma[k])/\overline{S}$ in (18). Substituting (30) in (28), the corresponding optimal rate adaptation is derived in (31), shown at the bottom of the next page. With a perfect CSI, i.e., $\rho = 1$, $\beta(\gamma'[k])$ degenerates to $\beta(\gamma[k])$ in (21). Finally, the exact analytical expression for the optimal ASE can be obtained

$$s\left(\gamma'[k]\right)/\overline{S} = \begin{cases} \frac{s_{\max}b+1}{\lambda(z)\ln(2)\overline{S}} - \frac{s_{\max}b+1}{\overline{S}a[\rho\gamma'[k]+(1-\rho)\overline{\gamma'[k]}\ln(\varepsilon/0.3)]}, & \gamma'_0 \le \gamma'[k] \le \gamma'_1 \quad \forall k \in \kappa \\ s_{\max}, & \gamma'[k] \ge \gamma'_1 \quad \forall k \in \kappa \end{cases} \tag{30}$$

by similar derivations performed in the perfect CSI case. The final result can be obtained as follows:

$$\begin{aligned} C_{\mathrm{ASE}'} &= \frac{1}{\ln(2)}\left(\exp(-\gamma_0'/\overline{S})\ln\left(X_1\gamma_0'+Y_1\right)\right.\\ &\qquad\left.+Ei\left(\left(1,\frac{X_1\gamma_0'+Y_1}{\overline{S}X_1}\right)\exp\left(Y_1/\left(X_1\overline{S}\right)\right)\right)\right)\\ &-\frac{1}{\ln(2)}\left(\exp(-\gamma_1'/\overline{S})\ln\left(X_1\gamma_1'+Y_1\right)\right.\\ &\qquad\left.+Ei\left(\left(1,\frac{X_1\gamma_1'+Y_1}{\overline{S}X_1}\right)\exp\left(Y_1/\left(X_1\overline{S}\right)\right)\right)\right)\\ &+\frac{1}{\ln(2)}\left(\exp(-\gamma_1'/\overline{S})\ln\left(X_2\gamma_1'+Y_2\right)\right.\\ &\qquad\left.+Ei\left(\left(1,\frac{X_2\gamma_1'+Y_2}{\overline{S}X_2}\right)\exp\left(Y_2/\left(X_2\overline{S}\right)\right)\right)\right) \end{aligned} \tag{32}$$

where

$$\begin{aligned} X_1 &= a\rho/\left(\ln(2)\lambda(z)\right)\\ Y_1 &= a(1-\rho)\overline{\gamma'[k]}\ln(\varepsilon/0.3)/\left(\ln(2)\lambda(z)\right)\\ X_2 &= a\rho\overline{S}s_{\max}/(1+s_{\max}b) = a\rho(1-z)\overline{S}/b\\ Y_2 &= \left(1+a(1-\rho)\overline{\gamma'[k]}\ln(\varepsilon/0.3)\overline{S}(1-z)/b\right). \end{aligned}$$

Evaluation of z and $\lambda(z)$ are also similar to the derivations presented in Section III. With perfect CSI, i.e., $\rho = 1$, then C'_{ASE} degenerates to C_{ASE} in (22).

V. Numerical Results and Discussions

We now investigate the performance of the power and rate adaptation schemes proposed in this paper numerically and by computer simulations.

In Fig. 2, the relationship between $s_{\max} = \lim_{\gamma[k]\to\infty}(s(\gamma[k])/\overline{S})$ and the CFO ν is presented. Note that the adaptive scheme proposed is conditionally adaptive when CFO, $\nu > 0$, and completely adaptive when $\nu = 0$. As shown in Fig. 2, when CFO is fixed, the value of $s_{\max}$ decreases monotonically as SNR increases. On the other hand, the optimal value of $s_{\max}$ decreases as the CFO increases when SNR is fixed. Consequently, the maximum spectral efficiency, which is obtained after the power and rate adaptation, decreases with $s_{\max}$. Similarly, regardless of the CFO level, the performance of the power and rate adaptation approaches the constant power adaptation (uniform power distribution) when $s_{\max}$ is close to 1 (SNR > 25 dB). At the same time, the uniform power distribution in constant power adaptation [5] is reached when $s_{\max} = 1$. Note that we can use $s_{\max}$ to explain why the rate and power adaptation result in only a little performance improvement relative to the uniform power distribution, particularly at high SNRs in [5]. Fig. 2 also indicates that our conditionally adaptive scheme can resist the impact of the CFO very effectively since $s_{\max}$ is almost unchanged with CFO, up to a certain level. The results also show that the improvement in the performance using the power and rate adaptation under high SNR or high CFO conditions is limited, compared with the uniform power distribution case.

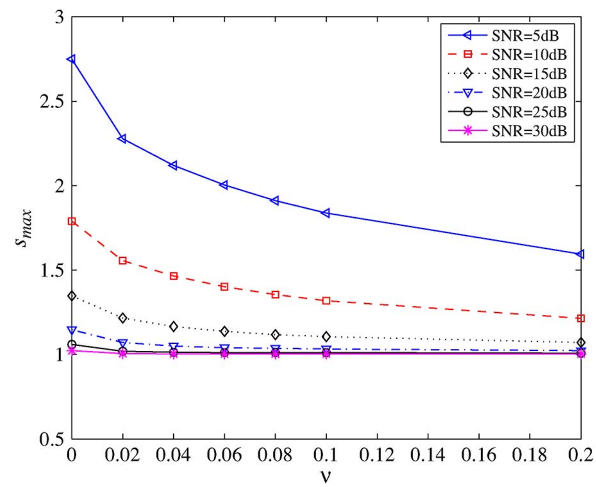

Fig. 2. Relationship between $s_{\max}$ and the carrier offset ν.

In Fig. 3, optimal power adaptation for different adaptive schemes are presented under perfect CSI and for different CFO values. As shown in Fig. 3, the curves of [19] are similar to the ones given by [5], particularly when CFO is small. Fig. 3 shows that the curves of the proposed conditional power adaptation consists of two parts, representing the complete adaptive scheme and the constant adaptation, respectively. We also observe that the conditional power adaptation scheme has the largest power $s_{\max} = \lim_{\gamma[k]\to\infty}(s(\gamma[k])/\overline{S})$ for all subcarriers. Therefore, the proposed scheme can meet the instantaneous BER constraint, and the higher CFO values result in a smaller range of $[\gamma_0, \gamma_1]$, implying that the optimal power adaptation adapts the constant power distribution over the high CFO values. However, $s_{\max}$ decreases as the CFO increases, which is equivalent to stating that the optimal power adaptation is close to the constant transmit power threshold $\gamma_0 \approx \gamma_1$ in [5] for large values of the CFO. Finally, we remark that our scheme also contains two special cases, namely, $s_{\max} = 1$ and CFO $= 0$, as discussed in [5] and [23].

$$\beta\left(\gamma'[k]\right) = \begin{cases} \log_2\left(\frac{a[\rho\gamma'[k]+(1-\rho)\overline{\gamma'[k]}\ln(\varepsilon/0.3)]}{\ln(2)\lambda(z)}\right), & {\gamma_0}' \le \gamma'[k] \le \gamma_1' \quad \forall k\in\kappa\\ \log_2\left(1+\frac{a[\rho\gamma'[k]+(1-\rho)\overline{\gamma'[k]}\ln(\varepsilon/0.3)]\overline{S}s_{\max}}{1+s_{\max}b}\right), & \gamma'[k] \ge {\gamma_1}' \quad \forall k\in\kappa \end{cases} \tag{31}$$

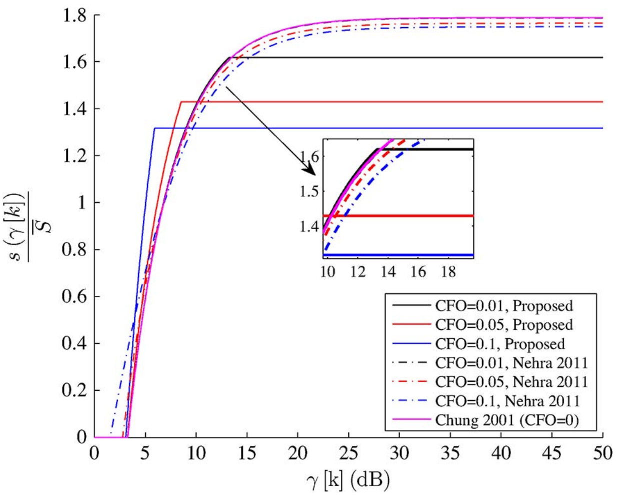

Fig. 3. $s(\gamma[k])/\overline{S}$ for different adaptive schemes ($\overline{\text{BER}} = 1^{-3}$, $\overline{\gamma[k]} =$ 10 dB) under perfect channel estimation conditions and different CFO values.

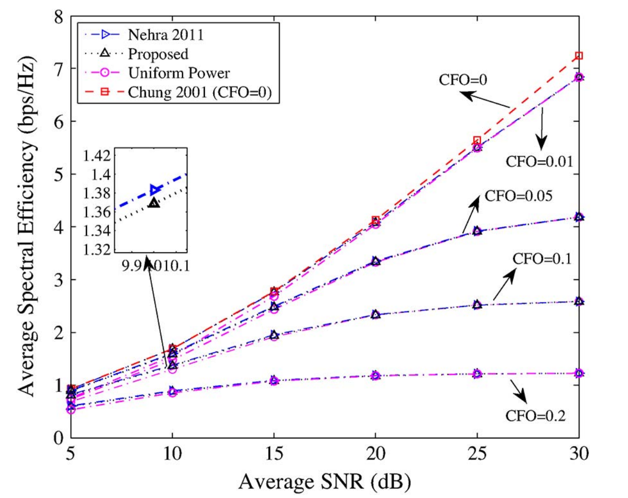

Fig. 5. ASE versus average SNR curves for different adaptive schemes under different CFO values.

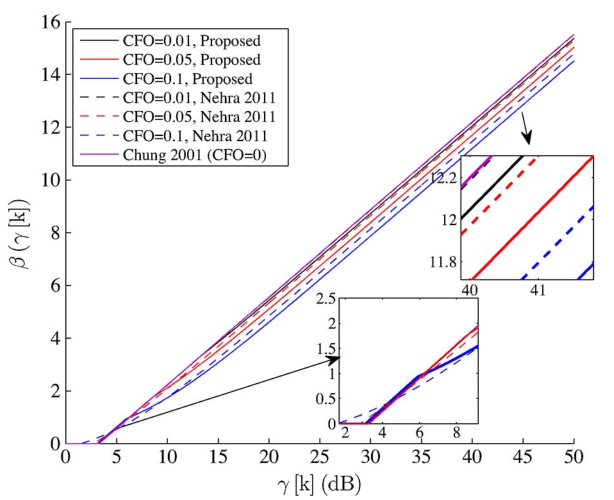

Fig. 4. $\beta(\gamma[k])$ for different adaptive schemes ($\overline{\text{BER}} = 10^{-3}$, $\overline{\gamma[k]} =$ 10 dB) under perfect channel estimation conditions and different CFO values.

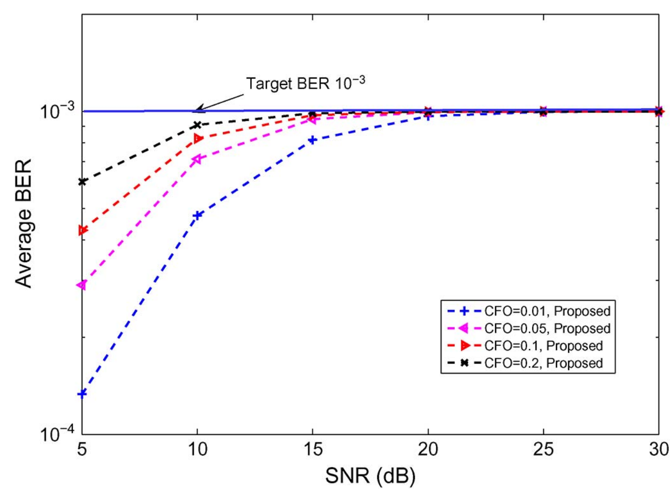

Fig. 6. Average BER versus SNR curves for different CFO values.

In Fig. 4, the bit rate adaptation $\beta(\gamma[k])$ is plotted as a function of $\gamma[k]$ for different adaptive schemes and for $\overline{\text{BER}} = 10^{-3}$ and $\overline{\gamma[k]} = 10$ dB under perfect channel estimation conditions and for different CFO values. Fig. 4 shows that the smaller CFO values yield larger bit rates than its higher CFO value counterparts when $\gamma[k]$ is fixed. The curves of [19] and of those presented in this paper, are close to the one given in [5], particularly when CFO is small. The Fig. 4 also shows that the bit rate curves consist of two parts. The first part has a higher slope than the second part, indicating that the difference of slopes increases with CFO.

In Fig. 5, the optimal ASE of the adaptive MQAM-OFDM system is plotted as a function of the average SNR, for the BER bound $\epsilon = 10^{-3}$ and for different CFO values under perfect CSI. The figure also shows the results of [5] and [19] with the same simulation parameters. We observe in Fig. 5 that the spectral efficiency of the system cannot be improved beyond a certain level, which is determined by the CFO values. This is mainly due to the contribution of the average SNR to the ICI power in the expression of effective SNR (7). In addition to this fact, we observe that the ASE performance of the uniform power and rate adaptation is very close to that of the optimal power and rate adaptation when SNR is high or for large CFO values. Therefore, improving the performance using the power and rate adaptation under high SNR or large CFO conditions is limited compared with the uniform power and rate adaptation.

Fig. 6 shows the average BER versus SNR curves for different CFO values with a target BER requirement of 10^{-3}. From the figure, we can see that our scheme meets the BER constraint for all the values of CFO and SNR.

In Fig. 7, the optimal power adaptation versus SNR is plotted for the case of MQAM signaling, i.e., $\overline{\text{BER}} = 10^{-3}$ and $\overline{\gamma[k]} =$ 10 dB, and for different CFO values under both perfect and imperfect channel estimation conditions. As shown in Fig. 7, the smaller correlation coefficient ρ (worse channel estimation error) results in a smaller range of $[\gamma_0, \gamma_1]$. This means that the optimal power adaptation tries to keep the constant power distribution even under poor channel estimation conditions. However, $s_{\max}$ increases as ρ decreases, mainly because the optimal power adaptation is close to the constant transmit power having threshold $\gamma_0 \approx \gamma_1$ in [5] with small ρ values.

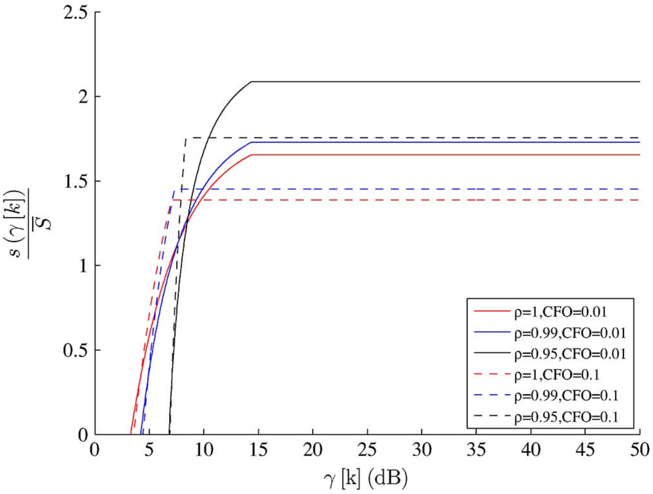

Fig. 7. $s(\gamma[k])/\overline{S}$ for adaptive continuous rate MQAM ($\overline{\text{BER}}=10^{-3}$, $\overline{\gamma[k]}=$ 10 dB) under different channel estimation conditions and different CFO values.

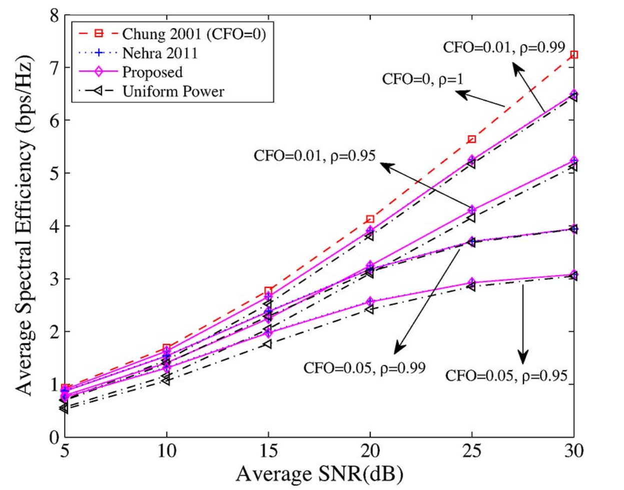

Fig. 9. ASE versus average SNR curves for different adaptive schemes with different channel estimation conditions under different CFO values.

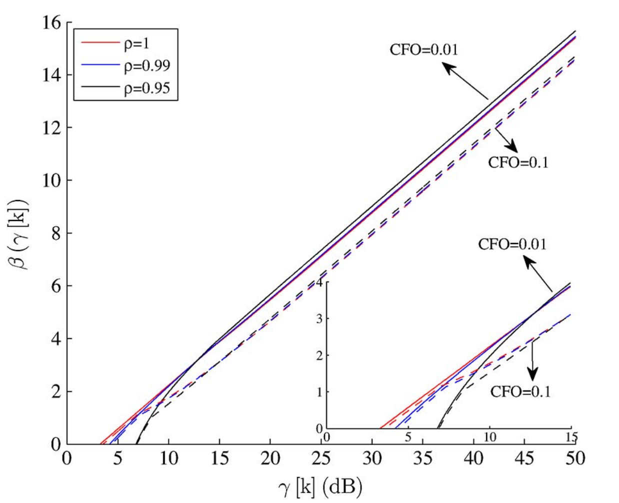

Fig. 8. $\beta(\gamma[k])$ for adaptive continuous rate MQAM ($\overline{\text{BER}}=10^{-3}$ and $\overline{\gamma[k]}=$ 10 dB) under different channel estimation conditions and different CFO values.

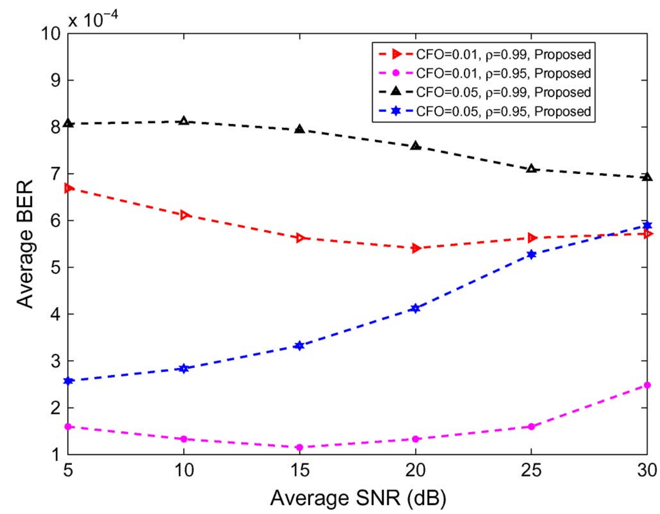

Fig. 10. Average BER versus SNR curves for proposed adaptive schemes with different channel estimation conditions under different CFO values.

In Fig. 8, the bit rate adaptation $\beta(\gamma[k])$ is plotted as a function of $\gamma[k]$ for the case of MQAM signaling, i.e., $\overline{\text{BER}} = 10^{-3}$ and $\overline{\gamma[k]} = 10$ dB, and for different CFO values under both perfect and imperfect CSI cases given (21) and (31), respectively. We observe that smaller CFO values yield larger bit rates when $\gamma[k]$ is fixed. Fig. 8 also shows that the bit rate curves have two parts with the first part has higher slope than the second part. Consequently, the bit rate decreases as ρ increases in $[\gamma_0, \gamma_1]$ and increases as ρ increases in $[\gamma_1, \infty]$ to guarantee the power constraint.

Fig. 9 shows the ASE of an adaptive MQAM OFDM system for different adaptive schemes with different CFO values under imperfect CSI. The figure shows that the proposed scheme is very close to the results presented in [19] with different CFO values and the channel estimation error ρ. The figure also indicates that an improvement in the performance with power and rate adaptation at high SNR or under CFO conditions is limited, as compared with that of the uniform power and rate adaptation scenarios.

Finally, Fig. 10 shows the average BER versus SNR curves for different adaptive schemes under different CFO values with imperfect CSI. From the figure, we can see that our scheme meets the BER constraint for all the values of CFO, irrespective of the CSI conditions.

VI. Conclusion

In this paper, the problem of power and rate adaptation has been investigated for MQAM/OFDM systems under CFO, with perfect and imperfect CSI. Under an instantaneous BER and average power constraints, optimal power and rate adaptation have been determined analytically to maximize the ASE for the system. Considering a target BER constraint for each subcarrier, a lower bound was derived, and closed-form expressions were obtained under channel estimation errors. The simulation results show that the SEA performance of the proposed scheme is valid because the performance almost achieves the upper bound of the method given by [19] and concluded that the ASE is seriously degraded under high CFO or imperfect channel estimations and that the performance cannot be improved beyond a certain level. The results also show that improving the performance using power and rate adaptation under high SNR or CFO is limited, compared with using uniform power and rate adaptation.

Appendix A
Solution of (17)

The optimization problem in (17) is not a convex program. It is rather a log-linear-fractional programming [24], [26]. However, we can transform it to a convex optimization problem by means of a linear-fractional programming as follows. Equation (17) can be expressed as

$$\text{maximize} \quad J(\mathbf{x}) = \int \log_2\left(\frac{\mathbf{c}^T\mathbf{x}+1}{\mathbf{e}^T\mathbf{x}+1}\right) p_{\gamma[k]}\left(\gamma[k]\right) d\gamma[k] \tag{33a}$$

subject to

$$E_{\gamma[k]}\{\mathbf{g}^T\mathbf{x}\} = \overline{S} \qquad \forall\, k \in \kappa \tag{33b}$$

$$\mathbf{g}^T\mathbf{x} \geq 0 \tag{33c}$$

$$\mathbf{d}^T\mathbf{x} \leq 0 \tag{33d}$$

$$\text{BER}\left(\gamma[k]\right) \leq \varepsilon \qquad \forall\, k \in \kappa \tag{33e}$$

where $s_{\max} \geq 1$, $\mathbf{x} = [s(\gamma[k]), s_{\max}]^T$, $\mathbf{c} = [a\gamma[k], b]^T$, $\mathbf{e} = [0, b]^T$, $\mathbf{g} = [1, 0]^T$, $\mathbf{d} = [1, -\overline{S}]^T$, and a, b are defined in (16). If the feasible set $\{\mathbf{x}|\mathbf{g}^T\mathbf{x} \geq 0,\ \mathbf{d}_T\mathbf{x} \leq 0,\ E_{\gamma[k]}\{\mathbf{g}^T\mathbf{x}\} = \overline{S}, \text{BER}([k]) \leq \varepsilon, \mathbf{e}^T\mathbf{x} + 1 > 0\}$ is nonempty, (33a)–(33d) can be transformed to an equivalent problem as follows [24], [25]:

$$\text{maximize} \quad \int \log_2(\mathbf{c}^T\mathbf{y} + z) p_{\gamma[k]}\left(\gamma[k]\right) d\gamma[k] \tag{34a}$$

subject to

$$E_{\gamma[k]}\{\mathbf{g}^T\mathbf{y}\} = z\overline{S} \qquad \forall\, k \in \kappa \tag{34b}$$

$$\mathbf{g}^T\mathbf{y} \geq 0 \tag{34c}$$

$$\mathbf{d}^T\mathbf{y} \leq 0 \tag{34d}$$

$$\mathbf{e}^T\mathbf{y} + z = 1 \tag{34e}$$

$$z \geq 0 \tag{34f}$$

$$\text{BER}\left(\gamma[k]\right) \leq \varepsilon \qquad \forall\, k \in \kappa \tag{34g}$$

with variables $\mathbf{y}$, z, where $\mathbf{y} = \mathbf{x}(\mathbf{e}^T\mathbf{x}+1)^{-1}$, and $z = (\mathbf{e}^T\mathbf{x}+1)^{-1} = (s_{\max}b+1)^{-1}$.

Proposition 1: If $(\mathbf{y}, \mathbf{z})$ is feasible in (33a)–(33e), with $z \neq 0$, then $\mathbf{x} = \mathbf{y}/z$ is feasible in (34a)–(34g), with the same objective value [24], [25].

Consequently, the log-linear-fractional programming stated in (33) is transformed to an equivalent log linear program in the form of (34), which is clearly a convex optimization problem [24].

Equations (34a)–(34g) can be simplified as

$$\max_{\{y_1(\gamma[k]),z\}} \int \log_2\left(1 + a\gamma[k]y_1\left(\gamma[k]\right)\right) p_{\gamma[k]}\left(\gamma[k]\right) d\gamma[k] \tag{35a}$$

subject to

$$E_{\gamma[k]}\left\{y_1\left(\gamma[k]\right)\right\} = z\overline{S} \qquad \forall\, k \in \kappa \tag{35b}$$

$$y_1\left(\gamma[k]\right) \geq 0 \qquad \forall\, k \in \kappa \tag{35c}$$

$$y_1\left(\gamma[k]\right) \leq (1-z)\overline{S}/b \qquad \forall\, k \in \kappa \tag{35d}$$

$$\text{BER}\left(\gamma[k]\right) \leq \varepsilon \qquad \forall\, k \in \kappa \tag{35e}$$

where $\mathbf{y} = [y_1(\gamma[k]), y_2]^T = [s(\gamma[k])/(\mathbf{e}^T\mathbf{x}+1), s_{\max}/(\mathbf{e}^T\mathbf{x}+1)]^T$, and $z = 1/(\mathbf{e}^T\mathbf{x}+1) = (1/(s_{\max}b+1)) > 0$. There is no gap between (34) and (35) when $z \neq 0$.

The Lagrangian of the optimization problem in (35a)–(35e) can be written as

$$\begin{aligned} J&\left\{y_1\left(\gamma[k]\right), z\right\} \\ &= \int \log_2\left[1 + a\gamma[k]y_1\left(\gamma[k]\right)\right] p_{\gamma[k]}\left(\gamma[k]\right) d\gamma[k] \\ &\quad - \lambda(z)\left(\int y_1\left(\gamma[k]\right) p_{\gamma[k]}\left(\gamma[k]\right) d\gamma[k] - z\overline{S}\right) \end{aligned} \tag{36}$$

where $\lambda(z)$ is the Lagrange multiplier, which is a function of z.

The optimal value of $y_1(\gamma[k])$ in (36) can be obtained by differentiating (36) with respect to $y_1(\gamma[k])$ and equating the derivative to zero. The resulting solution is given by

$$\begin{aligned} y_{1,\text{opt}}&\left(\gamma[k]\right) \\ &= \begin{cases} \frac{1}{\ln(2)\lambda(z)} - \frac{1}{a\gamma[k]}, & f_0 \leq \gamma[k] \leq f_1 \qquad \forall k \in \kappa \\ (1-z)\overline{S}/b, & \gamma[k] \geq f_1 \qquad \forall k \in \kappa \end{cases} \end{aligned} \tag{37}$$

where f_0 and f_1 are the optimized thresholds for $\gamma[k]$ such that, below f_0, the channel is not used, and above f_1, the channel is used with some fixed transmit power. They are determined from the constraint equations (35c) and (35d) as

$$f_0 = \ln(2)\lambda(z)/a, \tag{38}$$

$$f_1 = \frac{1}{a\left(1/\left(\ln(2)\lambda(z)\right) - (1-z)\overline{S}/b\right)}. \tag{39}$$

Next, we determine the optimal value of z. After substituting $y_{1,\text{opt}}(\gamma[k])$ in (36) for $y_1(\gamma[k])$, the resulting Lagrangian is stated as follows:

$$\begin{aligned} \psi(z) &\equiv J\left(y_{1,\text{opt}}\left(\gamma[k]\right), z\right) \\ &= \int \log_2\left(1 + a\gamma[k]y_{1,\text{opt}}\left(\gamma[k]\right)\right) p_{\gamma[k]}\left(\gamma[k]\right) d\gamma[k]. \end{aligned} \tag{40}$$

For $\gamma[k]$ having an exponential distribution with mean $\overline{\gamma}$, we can take the integral above over $\gamma[k] \in [f_0, f_1]$ and $\gamma[k] \in$

$[f_1, \infty]$, analytically as follows:

$$\begin{aligned}\psi(z) &= \frac{1}{\ln(2)}\exp(-f_0/\overline{S}) \\ &\quad\times\left(\ln\left(f_0 a/\left(\ln(2)\lambda(z)\right)\right)+Ei(1,f_0/\overline{S})\exp(f_0/\overline{S})\right) \\ &\quad-\frac{1}{\ln(2)}\exp(-f_1/\overline{S}) \\ &\quad\times\left(\ln\left(f_1 a/\left(\ln(2)\lambda(z)\right)\right)+Ei(1,f_1/\overline{S})\exp(f_1/\overline{S})\right) \\ &\quad+\frac{\exp(-f_1/\overline{S})}{\ln(2)} \\ &\quad\times\left(\log(1+Cf_1)+Ei\left(1,\frac{1+Cf_1}{C\overline{S}}\right)\exp\left(1+\frac{1+Cf_1}{C\overline{S}}\right)\right).\end{aligned} \tag{41}$$

We now show by the following proposition that $\psi(z)$ is a convex function of z. Therefore, the optimal value of z maximizing $\psi(z)$ can be easily determined.

Proposition 2: Suppose h is convex. Then, the function g defined by

$$g(x) = \inf\{h(y)|Ay = x\}$$

is convex [24].

It is clear that

$$J\left(y_1\left(\gamma[k]\right)\right) = \int \log_2\left(1 + a\gamma[k]y_1\left(\gamma[k]\right)\right)p_{\gamma[k]}\left(\gamma[k]\right)d\gamma[k]$$

is concave. Then, based on Proposition 2

$$\psi(z) = \sup\left\{J\left(y_1\left(\gamma[k]\right)\right)|E_{\gamma[k]}\left\{y_1\left(\gamma[k]\right)\right\} = z\overline{S}\right\}$$

is also concave. Consequently, the optimal z can be obtained from $\partial\psi(z)/\partial z = 0$. The derivative of $\psi(z)$ with respect to z can be taken from (41), as shown in (42), shown at the bottom of the page. where $C = a(1-z)\overline{S}/b$, and $\partial C/\partial z = -a\overline{S}/b$.

On the other hand, the Lagrangian multiplier $\lambda(z)$ can be determined from the constraint equation (35b), i.e.,

$$\begin{aligned}&\frac{\exp(-f_0/\overline{S})}{\ln(2)\lambda(z)} - Ei(1,f_0/\overline{S})/(a\overline{S}) - \frac{\exp(-f_1/\overline{S})}{\ln(2)\lambda(z)} - z\overline{S} \\ &\quad+ Ei(1,f_1/\overline{S})/(a\overline{S}) + \overline{S}\exp(-f_1/\overline{S})(1-z)/b = 0.\end{aligned} \tag{43}$$

Finally, the optimal power adaptation can be obtained by solving (36), shown in (44) at the bottom of the page, where z, from which $s_{\max}$, and $\lambda(z)$ are determined by solving equations in (45), shown at the bottom of the page, numerically using the "fsolve" command of Maple [27].

Appendix B
Derivation of (22)

$$\begin{aligned}C_{\text{ASE}} &= \int_{\gamma_0}^{\gamma_1}\log_2\left(\frac{a\gamma[k]}{\lambda(z)\ln(2)}\right)p_{\gamma[k]}\left(\gamma[k]\right)d\gamma[k] \\ &\quad+\int_{\gamma_1}^{\infty}\log_2\left(1+\frac{s_{\max}a\overline{S}\gamma[k]}{1+s_{\max}b}\right)p_{\gamma[k]}\left(\gamma[k]\right)d\gamma[k] \\ &= \int_{\gamma_0}^{\infty}\log_2\left(\frac{a\gamma[k]}{\lambda(z)\ln(2)}\right)p_{\gamma[k]}\left(\gamma[k]\right)d\gamma[k] \\ &\quad-\int_{\gamma_1}^{\infty}\log_2\left(\frac{a\gamma[k]}{\lambda(z)\ln(2)}\right)p_{\gamma[k]}\left(\gamma[k]\right)d\gamma[k] \\ &\quad+\int_{\gamma_1}^{\infty}\log_2\left(1+\frac{s_{\max}a\overline{S}\gamma[k]}{1+s_{\max}b}\right)p_{\gamma[k]}\left(\gamma[k]\right)d\gamma[k]\end{aligned} \tag{46}$$

$$\begin{aligned}\frac{\partial\psi(z)}{\partial z} &= -\left(\frac{\partial f_0}{\partial z}\right)\exp(-f_0/\overline{S})\log(f_0 a/(\ln(2)\lambda(z))) + \exp(-f_0/\overline{S})\left(\frac{\partial f_0}{\partial z}a\Big/(\ln(2)\lambda(z)) - f_0 a\left(\frac{\partial\lambda(z)}{\partial z}\right)\Big/\left(\ln(2)\lambda^2(z)\right)\right) \\ &\quad\times\ln(2)\lambda(z)/(f_0 a) - \frac{\partial f_0}{\partial z}\exp(-f_0/\overline{S})/f_0 + \left(\frac{\partial f_1}{\partial z}\right)\exp(-f_1/\overline{S})\log\left(f_1 a/\left(\ln(2)\lambda(z)\right)\right) - \exp(-f_1/\overline{S}) \\ &\quad\times\left(\frac{\partial f_1}{\partial z}a\Big/\left(\ln(2)\lambda(z)\right) - f_1 a\left(\frac{\partial\lambda(z)}{\partial z}\right)\Big/\left(\ln(2)\lambda^2(z)\right)\ln(2)\lambda(z)/(f_1 a) + \frac{\partial f_1}{\partial z}\exp(-f_1/\overline{S})/f_1\right. \\ &\quad-\exp(-f_1/\overline{S})\left(C^2\left(\frac{\partial f_1}{\partial z}\right)\log(1+Cf_1) - C\overline{S}\frac{\partial C}{\partial z} + Ei\left(1,\frac{1+Cf_1}{C\overline{S}}\right)\exp\left(1+\frac{1+Cf_1}{C\overline{S}}\right)\frac{\partial C}{\partial z}\right)\end{aligned} \tag{42}$$

$$\frac{s\left(\gamma[k]\right)}{\overline{S}} = \frac{y_1\left(\gamma[k]\right)}{z\overline{S}} = \begin{cases}\frac{1}{\ln(2)\lambda(z)} - \frac{1}{a\gamma[k]} = \frac{s_{\max}b+1}{\ln(2)\lambda(z)\overline{S}} - \frac{s_{\max}b+1}{a\gamma[k]\overline{S}}, & f_0 \le \gamma[k] \le f_1 \quad \forall\, k \in \kappa \\ s_{\max}, & \gamma[k] \ge f_1 \quad \forall\, k \in \kappa\end{cases} \tag{44}$$

$$\begin{cases}\frac{\exp(-f_0/\overline{S})}{\ln(2)\lambda(z)} - Ei(1,f_0/\overline{S})/(a\overline{S}) - \frac{\exp(-f_1/\overline{S})}{\ln(2)\lambda(z)} + Ei(1,f_1/\overline{S})/(a\overline{S}) + \overline{S}\exp(-f_1/\overline{S})(1-z)/b - z\overline{S} = 0 \\ \frac{\partial\psi(z)}{\partial z} = 0\end{cases} \tag{45}$$

$$
\begin{aligned}
C_{\mathrm{ASE}'} &= \int_{\gamma_0'}^{\gamma_1'} \log_2\left(\frac{a[\rho\gamma'[k] + (1-\rho)\overline{\gamma'[k]}\ln(\varepsilon/0.3)]}{\ln(2)\lambda(z)}\right) p_{\gamma'[k]}\left(\gamma'[k]\right) d\gamma'[k] \\
&\quad + \int_{\gamma_1'}^{\infty} \log_2\left(1 + \frac{a[\rho\gamma'[k] + (1-\rho)\overline{\gamma'[k]}\ln(\varepsilon/0.3)]\overline{S}s_{\max}}{1+s_{\max}b}\right) p_{\gamma'[k]}\left(\gamma'[k]\right) d\gamma'[k] \\
&= \frac{1}{\ln(2)}\left(\exp(-\gamma_0'/\overline{S})\ln\left(X_1\gamma_0' + Y_1\right) + Ei\left(\left(1, \frac{X_1\gamma_0' + Y_1}{\overline{S}X_1}\right)\exp\left(Y_1/\left(X_1\overline{S}\right)\right)\right)\right) \\
&\quad - \frac{1}{\ln(2)}\left(\exp(-\gamma_1'/\overline{S})\ln\left(X_1\gamma_1' + Y_1\right) + Ei\left(\left(1, \frac{X_1\gamma_1' + Y_1}{\overline{S}X_1}\right)\exp\left(Y_1/\left(X_1\overline{S}\right)\right)\right)\right) \\
&\quad + \frac{1}{\ln(2)}\left(\exp(-\gamma_1'/\overline{S})\ln\left(X_2\gamma_1' + Y_2\right) + Ei\left(\left(1, \frac{X_2\gamma_1' + Y_2}{\overline{S}X_2}\right)\exp\left(Y_2/\left(X_2\overline{S}\right)\right)\right)\right)
\end{aligned} \tag{48}
$$

---

where $C = s_{\max}a\overline{S}/(1+s_{\max}b) = a(1-z)\overline{S}/b$, z, and $\lambda(z)$ can be calculated in Appendix A. By means of the integral formula [28] $Ei(1,x) = \int_x^{\infty}(\exp(-t)/t)\,dt$, the following can be derived easily:

$$
\begin{aligned}
&\int_{\beta}^{\infty} \ln(\chi t)\exp(-ut)\,dt \\
&\quad = \frac{1}{u}\left(\ln(\chi\beta) \times \exp(-\beta u) + Ei(1,\beta u)\right) \\
&\int_{a}^{\infty} \ln(\chi t + 1)\exp(-ut)\,dt \\
&\quad = \frac{1}{u}\left(\ln(\chi a + 1) \times \exp(-au) \right.\\
&\qquad\quad \left. + Ei\left(1, \frac{u(\chi a+1)}{\chi}\right)\exp\left(\frac{u}{\chi}\right)\right) \\
&\int_{a}^{\infty} \ln(\chi t + d) \times \exp(-ut)\,dt \\
&\quad = \frac{1}{u}\left(\ln(\chi a + d) \times \exp(-au) \right.\\
&\qquad\quad \left. + Ei\left(1, \frac{u(\chi a+d)}{\chi}\right)\exp\left(\frac{ud}{\chi}\right)\right).
\end{aligned}
$$

We then obtain the final result as follows:

$$
\begin{aligned}
C_{\mathrm{ASE}} &= \frac{1}{\ln(2)}\exp(-\gamma_0/\overline{S})(\ln(\gamma_0 a/(\ln(2)\lambda(z))) \\
&\quad + Ei(1,\gamma_0/\overline{S})\exp(\gamma_0/\overline{S}) - \frac{1}{\ln(2)}\exp(-\gamma_1/\overline{S}) \\
&\quad \times (\ln(\gamma_1 a/(\ln(2)\lambda(z))) + Ei(1,\gamma_1/\overline{S})\exp(\gamma_1/\overline{S})) \\
&\quad + \frac{\exp(-\gamma_1/\overline{S})}{\ln(2)} \\
&\quad \times \left(\log(1+C\gamma_1) + Ei\left(1, \frac{1+C\gamma_1}{C\overline{S}}\right) \right.\\
&\qquad \left. \times \exp\left(1 + \frac{1+C\gamma_1}{C\overline{S}}\right)\right).
\end{aligned} \tag{47}
$$

Closed-form expressions of (32) can be obtained by a similar approach as in (48), shown at the top of page, where

$$
\begin{aligned}
X_1 &= a\rho/(\ln(2)\lambda(z)) \\
Y_1 &= a(1-\rho)\overline{\gamma'}[k]\ln(\varepsilon/0.3)/\left(\ln(2)\lambda(z)\right) \\
X_2 &= a\rho\overline{S}s_{\max}/(1+s_{\max}b) = a\rho(1-z)\overline{S}/b \\
Y_2 &= \left(1 + a\left(1-\rho\right)\overline{\gamma'[k]}\ln(\varepsilon/0.3)\overline{S}(1-z)/b\right).
\end{aligned}
$$

ACKNOWLEDGMENT

The authors would like to thank the anonymous reviewers for their comments and suggestions, which helped to significantly improve the quality of this paper.

REFERENCES

[1] R. Prasad, *OFDM for Wireless Communications Systems*. Norwood, MA, USA: Artech House, 2004.

[2] P. Moose, "A technique for orthogonal frequency division multiplexing frequency offset correction," *IEEE Trans. Commun.*, vol. 42, no. 10, pp. 2908–2914, Oct. 1994.

[3] H. Cheon and D. Hong, "Effect of channel estimation error in OFDM-based WLAN," *IEEE Commun. Lett.*, vol. 6, no. 5, pp. 190–192, May 2002.

[4] L. Rugini and P. Banelli, "BER of OFDM systems impaired by carrier frequency offset in multipath fading channels," *IEEE Trans. Wireless Commun.*, vol. 4, no. 5, pp. 2279–2288, Sep. 2005.

[5] S. Chung and A. Goldsmith, "Degrees of freedom in adaptive modulation: A unified view," *IEEE Trans. Commun.*, vol. 49, no. 9, pp. 1561–1571, Sep. 2001.

[6] C. Liu, D. Bielefeld, and R. Mathar, "Optimal rate and power allocation for OFDM in the presence of channel uncertainty," in *Proc. IEEE PIMRC*, Sep. 2008, pp. 1–5.

[7] Z. Mao and X. Wang, "Efficient optimal and suboptimal radio resource allocation in OFDMA system," *IEEE Trans. Wireless Commun.*, vol. 7, no. 2, pp. 440–445, Feb. 2008.

[8] J. Huang, V. Subramanian, R. Agrawal, and R. Berry, "Downlink scheduling and resource allocation for OFDM systems," *IEEE Trans. Wireless Commun.*, vol. 8, no. 1, pp. 288–296, Jan. 2009.

[9] X. Yu, S. Leung, W. Mow, and W. Wong, "Performance of variable-power adaptive modulation with space-time coding and imperfect CSI in MIMO systems," *IEEE Trans. Veh. Technol.*, vol. 58, no. 4, pp. 2115–2120, May 2009.

[10] X. Tang, M. Alouini, and A. Goldsmith, “Effect of channel estimation error on M-QAM BER performance in Rayleigh fading,” *IEEE Trans. Commun.*, vol. 47, no. 12, pp. 1856–1864, Jul. 1999.

[11] S. Ye, R. Blum, and L. Cimini, “Adaptive OFDM systems with imperfect channel state information,” *IEEE Trans. Wireless Commun.*, vol. 5, no. 11, pp. 3255–3265, Nov. 2006.

[12] A. Olfat and M. Shikh-Bahaei, “Optimum power and rate adaptation for MQAM in Rayleigh flat fading with imperfect channel estimation,” *IEEE Trans. Veh. Technol.*, vol. 57, no. 4, pp. 2622–2627, Jul. 2008.

[13] S. Das, E. De Carvalho, and R. Prasad, “Performance analysis of OFDM systems with adaptive sub carrier bandwidth,” *IEEE Trans. Wireless Commun.*, vol. 7, no. 4, pp. 1117–1122, Apr. 2008.

[14] J. Wen, C. Chiang, T. Hsu, and H. Hung, “Resource management techniques for ofdm systems with the presence of inter-carrier interference,” *Wireless Pers. Commun.*, vol. 65, no. 3, pp. 515–535, Apr. 2011.

[15] Y. Ma, “Rate maximization for downlink OFDMA with proportional fairness,” *IEEE Trans. Veh. Technol.*, vol. 57, no. 5, pp. 3267–3274, Sep. 2008.

[16] W. W. Ho and Y.-C. Liang, “Optimal resource allocation for multiuser MIMO-OFDM systems with user rate constraints,” *IEEE Trans. Veh. Technol.*, vol. 58, no. 3, pp. 1190–1203, Mar. 2009.

[17] Z. Dong, P. Fan, E. Panayirci, and P. Mathiopoulos, “Effect of power and rate adaptation on the spectral efficiency of MQAM/OFDM system under very fast fading channels,” *EURASIP J. Wireless Commun. Netw.*, vol. 2012, no. 1, p. 208, Jul. 2012.

[18] Z. Dong, P. Fan, W. Zhou, and E. Panayirci, “Power and rate adaptation for MQAM/OFDM systems under fast fading channels,” in *Proc. IEEE Veh. Technol. Conf.*, May 2012, pp. 1–5.

[19] K. Nehra and M. Shikh-Bahaei, “Spectral efficiency of adaptive MQAM/OFDM systems with CFO over fading channels,” *IEEE Trans. Veh. Technol.*, vol. 60, no. 3, pp. 1240–1247, Mar. 2011.

[20] T. Vo, K. Amis, T. Chonavel, and P. Siohan, “Achievable throughput optimization in OFDM systems in the presence of interference and its application to power line networks,” *IEEE Trans. Commun.*, vol. 62, no. 5, pp. 1704–1715, May 2014.

[21] A. Garcia Armada, “Understanding the effects of phase noise in orthogonal frequency division multiplexing (OFDM),” *IEEE Trans. Broadcast.*, vol. 47, no. 2, pp. 153–159, Jun. 2001.

[22] M. K. Simon and M.-S. Alouini, *Digital Communication Over Fading Channels*, vol. 95, Hoboken, NJ, USA: Wiley, 2005.

[23] A. J. Goldsmith and S.-G. Chua, “Variable-rate variable-power MQAM for fading channels,” *IEEE Trans. Commun.*, vol. 45, no. 10, pp. 1218–1230, Oct. 1997.

[24] S. Boyd and L. Vandenberghe, *Convex Optimization*. Cambridge, U.K.: Cambridge Univ. Press, 2004.

[25] A. Charnes and W. W. Cooper, “Programming with phlinear phfractional phfunctionals,” *Naval Res. Logist. Quart.*, vol. 9, no. 3/4, pp. 181–186, Sep. 1962.

[26] A. Chiang and K. Wainwright, *Fundamental Methods of Mathematical Economics*. New York, NY, USA: McGraw-Hill, 2005.

[27] C. S. Tocci and S. Adams, *Applied Maple for Engineers and Scientists*. Norwood, MA, USA: Artech House, 1996.

[28] I. Gradshten, I. Ryzhik, A. Jeffrey, and D. Zwillinger, *Table of Integrals, Series and Products*, 7th ed., San Diego, CA, USA: Academic, 2007.

Zhicheng Dong (S’12) was born in Langzhong, China, in 1982. He received the B.E. and M.S. degrees from Southwest Jiaotong University, Chengdu, China, in 2004 and 2008, respectively. He is currently working toward the Ph.D. degree with the Key Laboratory of Information Coding and Transmission, Southwest Jiaotong University.

He is also currently with the School of Engineering, Tibet University, Lhasa, China. His research interests include adaptation technology, performance analysis, and signal processing for high-mobility wireless communications.

Mr. Dong has served/will serve as a Technical Program Committee member for the International Conference on Communications and Networking in China in 2014 and the IEEE International Conference on Communications in 2015.

Pingzhi Fan (M’93–SM’99–F’15) received the Ph.D. degree in electronic engineering from Hull University, Hull, U.K.

He is currently a Professor and a Director of the Institute of Mobile Communications, Southwest Jiaotong University, Leshan, China. He was a Chief Scientist of a 973 research project. He is the author of around 200 research papers published in various academic English journals (IEEE/IEE/IEICE, etc.) and eight books (including edited) published by John Wiley and Sons (1996), IEEE Press (2011, etc.), Springer (2004), and Nova Science (2007) and is the inventor of 20 granted Patent Cooperation Treaty and Chinese patents. His publications have received over 5000 citations (Google Scholar). His research interests include high-mobility wireless communications, spread-spectrum techniques, and signal design and coding.

Dr. Fan has served as a General Chair or a Technical Program Committee Chair of a number of international conferences and as a Guest Editor-In-Chief, a Guest Editor, or an editorial board member for several international journals. He is the Founding Chair of the IEEE Vehicular Technology Society Beijing Chapter and the Founding Chair of IEEE Chengdu Section. He also served as a board member of IEEE Region 10, IET (IEE) Council, and IET Asia-Pacific Region. He received the U.K. Overseas Research Students Award and the Outstanding Young Scientist Award from the National Natural Science Foundation of China.

Erdal Panayirci (M’80–SM’91–F’03–LF’06) received the Engineer Diploma in electrical engineering from Istanbul Technical University, Istanbul, Turkey, and the Ph.D. degree in electrical engineering and system science from Michigan State University, East Lansing, MI, USA.

Until 1998, he was with the Faculty of Electrical and Electronics Engineering, Istanbul Technical University, where he was a Professor and Head of the Telecommunications Chair. He spent the academic year 2008–2009 with the Department of Electrical Engineering, Princeton University, NJ, USA, working on new channel estimation and equalization algorithms for high-mobility Worldwide Interoperability for Microwave Access and Long-Term Evolution systems. He is currently a Professor of electrical engineering and the Head of the Department of Electronics Engineering, Kadir Has University, Istanbul. He has been the Principal Coordinator of the Sixth and Seventh Frame European Projects called the Network of Excellent on Wireless Communications (NEWCOM), representing Kadir Has University for five years, and the WIMAGIC Strep project for two years. He is currently the Head of the Turkish Scientific Commission on Signals and Systems for the International Union of Radio Science. He has published extensively in leading scientific journals and international conferences and is the coauthor of *Principles of Integrated Maritime Surveillance Systems* (Boston, MA, USA, Kluwer, 2000) His research interests include communication theory, synchronization, advanced signal processing techniques and their applications to wireless communications, coded modulation, and interference cancelation in heterogeneous networks.

Dr. Panayirci served as a Member of the IEEE Fellow Committee during 2005–2008. He served as the Technical Program Cochair for the IEEE International Conference on Communications in 2006 and the Technical Program Chair of the IEEE International Symposium on Personal, Indoor, and Mobile Radio Communications in 2010, both held in Istanbul. He was the Executive Vice Chair of the 2014 IEEE Wireless Communications and Networking Conference. He was an Editor for IEEE TRANSACTIONS ON COMMUNICATIONS in the areas of synchronization and equalizations during 1995–1999.

Xianfu Lei (M'13) was born in December 1981. He received the Ph.D. degree in communication and information systems from Southwest Jiaotong University, Chengdu, China, in 2012.

Since December 2012, he has been a Research Fellow with the Department of Electrical and Computer Engineering, Utah State University, Logan, UT, USA. He has more than 50 journal and conference papers. His current research interests include wireless communication theory, cooperative communications, cognitive radio, physical-layer security, energy harvesting, heterogeneous networks, and millimeter-wave communications.

Dr. Lei currently serves on the Editorial Board of IEEE COMMUNICATIONS LETTERS and *Wiley Security and Communication Networks*. He is currently the Lead Guest Editor of the special issue on energy harvesting wireless communications for the *EURASIP Journal on Wireless Communications and Networking*. He also served as a Technical Program Committee member for major international conferences such as the IEEE International Conference on Communications; the IEEE Global Communications Conference; the IEEE Wireless Communications and Networking Conference; the IEEE Spring/Fall Vehicular Technology Conference; the IEEE International Symposium on Personal Indoor, Mobile, and Radio Communications, etc. He received an Exemplary Reviewer Certificate from the IEEE COMMUNICATIONS LETTERS and an Exemplary Reviewer Certificate from the IEEE WIRELESS COMMUNICATIONS LETTERS in 2013.